environments

MDPI

Article

Radiolytic Breakdown of PFOS by Neutron Irradiation: Mechanistic Insights into Molecular Disassembly and Cytotoxicity Reduction

Jéssica Ingrid Faria de Souza [1,2], Pierre Basilio Almeida Fechine [3], Eduardo Ricci-Junior [4], Luciana Magalhães Rebelo Alencar [5], Júlia Fernanda da Costa Araújo [6], Severino Alves Junior [6] and Ralph Santos-Oliveira [1,2,*]

1 Laboratory of Nanoradiopharmacy and Synthesis of New Radiopharmaceuticals, Nuclear Engineering Institute, Brazilian Nuclear Energy Commission, Rua Hélio de Almeida, 75, Ilha do Fundão, Rio de Janeiro 21941906, RJ, Brazil; jessicaifaria@gmail.com
2 Laboratory of Radiopharmacy and Nanoradiopharmaceuticals, Rio de Janeiro State University, Rio de Janeiro 23070200, RJ, Brazil
3 Grupo de Química de Materiais Avançados (GQMat), Departamento de Química Analítica e Físico-Química, Universidade Federal do Ceará–UFC, Campus do Pici, Fortaleza 60451970, CE, Brazil; fechine@ufc.br
4 School of Pharmacy, Federal University of Rio de Janeiro, Rio de Janeiro 21941900, RJ, Brazil; ricci@pharma.ufrj.br
5 Biophysics and Nanosystems Laboratory, Department of Physics, Federal University of Maranhão, São Luis 65065690, MA, Brazil; luciana.alencar@ufma.br
6 Department of Fundamental Chemistry, Federal University of Pernambuco, Recife 50670901, PE, Brazil; julia.fernandaarauajo@gmail.com (J.F.d.C.A.); salvesjr@ufpe.br (S.A.J.)
* Correspondence: roliveira@ien.gov.br or presidenciaradiofarmacia@gmail.com

Abstract

Perfluorooctane sulfonate (PFOS), a persistent and bioaccumulative perfluoroalkyl substance, poses significant environmental and human health risks due to the extraordinary stability of its C–F bonds. Conventional remediation strategies largely fail to achieve mineralization, instead transferring contamination or producing secondary waste streams. In this study, we investigate neutron irradiation as a potential destructive approach for PFOS remediation in both solid and aqueous matrices. Samples were exposed to thermal neutrons (flux: 3.2×10^9 n·cm^{-2}·s^{-1}, 0.0025 eV) at the Argonauta reactor for 6 h. Raman and FTIR spectroscopy revealed that PFOS in powder form remained largely resistant to degradation, with only minor structural perturbations observed. In contrast, aqueous PFOS solutions exhibited pronounced spectral changes, including attenuation of C–F and S–O vibrational signatures, the emergence of carboxylate and carbonyl functionalities, and enhanced O–H stretching, consistent with radiolytic oxidation and partial defluorination. Notably, clear peak shifts were predominantly observed for PFOS in aqueous solution after irradiation (overall displacement toward higher wavenumbers), whereas in powdered PFOS the main spectral signature of irradiation was the attenuation of CF_2 and S–O related bands with comparatively limited band relocation. To evaluate the biological relevance of these structural alterations, cell viability assays (MTT) were performed using human umbilical vein endothelial cells. Non-irradiated PFOS induced marked cytotoxicity at 100 and 50 µg/mL ($p < 0.0001$), whereas neutron-irradiated PFOS no longer exhibited significant toxicity, with cell viability comparable to the control. These findings indicate a matrix-dependent response: neutron scattering in solids yields negligible molecular breakdown, whereas radiolysis-driven pathways in water facilitate measurable PFOS transformation. The cytotoxicity assay demonstrates that neutron irradiation promotes sufficient molecular degradation of PFOS in aqueous media to suppress its cytotoxic effects. Although complete mineralization was not achieved under the tested conditions, the combined spectroscopic

Check for updates

Academic Editors: Frank Gobas and Petros A. Kokkinos

Received: 18 November 2025
Revised: 25 December 2025
Accepted: 8 January 2026
Published: 11 January 2026

Copyright: © 2026 by the authors. Licensee MDPI, Basel, Switzerland. This article is an open access article distributed under the terms and conditions of the Creative Commons Attribution (CC BY) license.

and biological evidence supports neutron-induced radiolysis as a promising pathway for perfluoroalkyl detoxification. Future optimization of neutron flux, irradiation duration, and synergistic catalytic systems may enhance mineralization efficiency. Because PFOS concentration, fluoride release (F^-), and TOC were not quantified in this study, remediation was assessed through spectroscopic fingerprints of transformation and the suppression of cytotoxicity, rather than by mass-balance mineralization metrics. This study highlights neutron irradiation as a promising strategy for perfluoroalkyl destruction in contaminated water sources.

Keywords: perfluorooctane sulfonate (PFOS); per- and polyfluoroalkyl substances; neutron irradiation; water radiolysis; Raman spectroscopy; FTIR; defluorination; cytotoxicity (HUVEC)

1. Introduction

Perfluorooctane sulfonate (PFOS) is one of the most widely used and studied perfluoroalkyl substances. It has been extensively employed in firefighting foams, stain-resistant textiles, non-stick coatings, lubricants, and surface protectants. Owing to its amphiphilic structure—perfluorinated hydrophobic tail and a sulfonate polar head—PFOS possesses unique surfactant properties that have made it indispensable in industry for decades [1,2].

However, the same structural features confer extraordinary stability. The carbon–fluorine (C–F) bond, one of the strongest in organic chemistry (≈485 kJ/mol) [3], resists hydrolysis, photolysis, biodegradation and conventional oxidation. Consequently, PFOS has become a global environmental contaminant, detected in surface water, groundwater, sediments, soil, and even remote polar regions [4,5]. It bioaccumulates in food webs and has been measured in fish, birds, marine mammals [6], and human serum [7].

Toxicological and epidemiological studies have consistently linked PFOS exposure to a wide range of adverse health effects through defined molecular mechanisms. Endocrine disruption is mediated by PFOS binding competitively to thyroid hormone transport proteins such as transthyretin, displacing thyroxine (T4) and altering thyroid receptor signaling [8]. In addition, PFOS interferes with steroidogenesis, reducing the synthesis of reproductive hormones [9]. Immunotoxicity arises from PFOS modulation of immune signaling pathways, including suppression of cytokine production and impaired activation of B and T lymphocytes, which lead to reduced vaccine response and weakened host defense [10]. In the case of metabolic disorders, PFOS activates peroxisome proliferator-activated receptor alpha (PPARα) and related nuclear receptors, altering lipid metabolism and hepatic gene expression, thereby promoting dyslipidemia, hepatic steatosis, and insulin resistance [11,12]. Carcinogenicity has been associated with chronic PFOS exposure through mechanisms including oxidative stress, mitochondrial dysfunction, and persistent PPARα activation, which collectively promote hepatocellular proliferation and increased risk of liver and kidney cancers [13,14]. Finally, developmental toxicity results from PFOS transfer across the placenta, where it interferes with endocrine regulation and growth factor pathways, leading to impaired fetal development, neurodevelopmental alterations, and reduced fertility.

Because PFOS exhibits a long elimination half-life in humans (≈5 years in serum), even low-level chronic exposure results in bioaccumulation and long-term systemic risk [15]. This persistence and bioaccumulative potential prompted international regulatory action, with PFOS listed under the Stockholm Convention on Persistent Organic Pollutants (2009) [16].

The environmental sources of PFOS contamination are diverse. The most significant are aqueous film-forming foams used in firefighting, which are major contributors to groundwater pollution near airports and military bases. Industrial discharges, including those from electroplating, textiles, and paper coatings, represent another important source [17,18]. Furthermore, wastewater treatment plants and landfill leachates fail to degrade PFOS effectively, instead redistributing it into effluents and biosolids [19]. Once released, PFOS is highly mobile in aquatic systems and poorly removed by adsorption or conventional filtration methods, allowing it to persist in aquifers, rivers, and oceans for decades. Its widespread detection globally underscores its long-range environmental transport and persistence [20–23].

Numerous approaches have been investigated for PFOS remediation, but each has critical limitations. Adsorption technologies (e.g., activated carbon, ion exchange resins) can efficiently capture PFOS but do not destroy it, merely transferring contamination to another phase, which requires further disposal [24]. Advanced oxidation processes, including UV/H_2O_2 and ozonation, are largely ineffective due to the high bond dissociation energy of the C–F bond [25]. Electrochemical oxidation shows promise in achieving mineralization of PFOS under optimized conditions, but is hampered by high energy requirements and electrode fouling, reducing long-term viability [26]. Plasma treatment and photocatalysis have demonstrated potential to break down PFOS under laboratory conditions, but issues of scalability and energy efficiency remain unresolved [27]. High-temperature incineration (>1100 °C) is currently the only fully destructive method applied in practice, but it is highly energy-intensive and poses risks of incomplete combustion, with possible generation of toxic by-products [28].

From a physicochemical standpoint, PFOS exhibits a unique combination of properties that underpin its environmental persistence and resistance to conventional remediation. The fully fluorinated carbon chain confers extreme hydrophobicity, chemical inertness, and thermal stability, while the sulfonate headgroup imparts strong acidity and surfactant behavior, promoting high solubility and mobility in aqueous environments. This dual character leads to strong adsorption at interfaces, bioaccumulation in protein-rich tissues, and poor removal by standard treatment processes. In addition, PFOS displays high thermal stability and low vapor pressure, further limiting degradation through conventional physical or chemical pathways [29,30].

Several advanced methods have been investigated to address PFOS persistence. Sonochemical treatment relies on acoustic cavitation to generate localized hot spots and reactive radicals capable of initiating C–F bond cleavage; however, its efficiency is often limited by energy demand and incomplete mineralization. Ozonation and other advanced oxidation processes, including UV/H_2O_2, typically fail to effectively degrade PFOS due to the exceptional bond dissociation energy of the C–F bond. Electrochemical oxidation and plasma-based technologies have demonstrated partial to near-complete degradation under optimized laboratory conditions, yet challenges related to electrode degradation, scalability, and energy efficiency remain. Ionizing radiation techniques, such as electron beam and γ-irradiation, have emerged as promising destructive approaches by inducing radiolysis-driven pathways in aqueous systems, motivating the exploration of neutron irradiation as a complementary and fundamentally distinct strategy for PFOS transformation [30–34].

Neutrons are charge-neutral subatomic particles with the unique ability to penetrate matter and interact directly with atomic nuclei, making them fundamentally different from charged particles that are deflected by electron clouds [35,36]. Their interactions include elastic and inelastic scattering, which alter atomic structure and can disrupt molecular stability; neutron capture, in which nuclei absorb neutrons and are converted into isotopes; and nuclear transmutation, where the identity of an atom is changed entirely, such as the

conversion of stable fluorine-19 (^{19}F) into other isotopes like ^{20}F or 1^{8F} [37]. These processes provide a theoretical foundation for exploring neutron-based strategies in the degradation of persistent contaminants such as PFOS.

The potential mechanisms by which neutrons could degrade PFOS center on disrupting the extraordinary stability of the C–F bond. Direct destabilization of C–F bonds could occur through interactions between neutrons and the fluorine nuclei, weakening the molecular framework and initiating fragmentation of the PFOS molecule [38]. A secondary radical generation is possible with neutron irradiation in aqueous environments. The radiolysis of water under neutron exposure produces highly reactive radicals such as hydroxyl (•OH) and hydrogen (•H), which can attack PFOS molecules and facilitate defluorination [39,40].

The advantages of such an approach are noteworthy. Neutron irradiation could, in principle, fully mineralize PFOS into carbon dioxide (CO_2), hydrogen fluoride (HF), and inorganic salts, eliminating rather than displacing contamination. Unlike conventional oxidative or adsorptive methods, this constitutes a direct nuclear-level approach targeting the elemental composition of PFOS. Furthermore, it may be particularly well suited for treating point-source contamination hotspots, such as groundwater near firefighting training sites heavily polluted with aqueous film-forming foams [35–37].

In this study, we have evaluated the effect of neutron irradiation on PFOS, both solid and dispersed in water in order to evaluate its feasibility remediating PFOS's presence in the environment.

Importantly, this study is presented as a proof-of-concept aimed at elucidating whether exposure to a reactor mixed-field environment can drive PFOS molecular transformations and reduce biological activity, rather than as a direct proposal for immediate large-scale environmental deployment. The novelty of the study lies in (i) reporting, to our knowledge, the first evaluation of PFOS exposed to thermal neutron irradiation under research-reactor conditions, and (ii) demonstrating a clear matrix-dependence, where solid PFOS remains largely resistant while aqueous PFOS exhibits radiolysis-consistent functional-group transformations coupled to reduced cytotoxicity.

2. Methodology

2.1. Neutron Irradiation

The neutron irradiation protocol was adopted from Dos Reis et al. [18]. Samples of 500 mg of PFOS, in both solid and aqueous solution forms, were irradiated at the Argonauta Reactor (Potency of 340 W) installed at the Nuclear Engineering Institute (Brazil). The samples were irradiated for 6 h using a thermal neutron flux of 3.2 $\times$ 109 $n \cdot cm^{-2} \cdot s^{-1}$ with average thermal neutron energy of 0.0025 eV. The thermal activation microscopic cross-section was 98.5 $\pm$ 0.4 barns.

2.2. In Vitro Cell Culture

Human umbilical vein endothelial cells were obtained from the Rio de Janeiro Cell Bank (BCRJ) and kept in DMEM-high medium supplemented with 10% (*v*/*v*) fetal bovine serum, 2 mM L-glutamine, and 1% (*v*/*v*) penicillin/streptomycin. The cells were cultured and expanded in T75 cm^2 flasks and maintained in a humidified incubator at 5% CO_2 and 37 °C. Monolayer assays were performed in 96-well flat-bottom plates.

2.3. Treatment with Perfluorooctane Sulfonate (PFOS)

After incubation, endothelial cells were cultured in 96-well plates at a concentration of 1 $\times$ 10^4 cells. After 24 h of adhesion, they were treated with concentrations of 3.125, 6.25, 12.5, 25, 50, and 100 µg/mL of irradiated and non-irradiated aqueous perfluorooctane

sulfonate solutions and incubated for 24 h. A death control was performed using the corresponding cell medium with 10% (*v*/*v*) Triton. The positive control corresponds to untreated cells cultured only in the cell culture medium.

2.4. Cell Viability Assay

To evaluate cytotoxicity in cell lines, we performed the MTT assay, based on Singh et al., 2015 [41]. At the end of the designated time, the MTT solution (Sigma-Aldrich®, St. Louis, MO, USA) was added at a concentration of 1 mg/mL to the culture and incubated for 3 h. After the incubation period, the formazan crystals were dissolved with DMSO, and the absorbance was measured by a multipartite spectrophotometer (Multiskan FC; Thermo Fisher Scientific Inc., Waltham, MA, USA) at a wavelength of 450 nm.

It should be noted that the present study prioritized spectroscopic techniques (Raman and FTIR) and biological assays to probe molecular integrity, functional group transformation, and cytotoxicity of PFOS following neutron irradiation. Complementary physicochemical techniques such as thermogravimetric analysis (TGA), Brunauer–Emmett–Teller (BET) surface area analysis, and scanning electron microscopy coupled with energy-dispersive X-ray spectroscopy (SEM–EDX) were not employed, as PFOS is a low-volatility molecular compound rather than a particulate or porous material. Nevertheless, TGA could provide additional insight into thermal stability changes following irradiation, while SEM–EDX and BET may be valuable for future studies involving PFOS immobilized on solid matrices, soils, or engineered adsorbents. These techniques will be considered in subsequent investigations aimed at heterogeneous environmental systems.

Accordingly, morphological metrics were not expected to be mechanistically decisive for these homogeneous aqueous experiments but will be essential in future work targeting PFOS in solids, soils, or PFOS-loaded sorbents.

3. Results

3.1. Powder PFOS—Raman and FTIR

The Raman spectrum of the material shows characteristic bands assigned to the vibrational modes of both the fluorinated polymeric backbone and the sulfonated moieties (Figure 1). The peak at 302 cm^{-1} was assigned to C–C and C–F stretching vibrations. The bands at 368 and 714 cm^{-1} correspond to CF_2 vibrations (wagging/rocking), confirming the presence of fluoroalkyl moieties within the polymer [42].

The spectral region between 559–654 cm^{-1} was attributed to O–S–O and C–S stretching vibrations, consistent with the presence of sulfonated groups [43]. Additionally, a peak at 876 cm^{-1} was assigned to S–O stretching, in agreement with reported data for sulfonic and fluorinated compounds [44].

At higher wavenumbers, the band at 1207 cm^{-1} was assigned to SO_2 vibrations, as well as to fluoroalkyl groups $–CF_2–$ and $–CF_3$. The peak at 1329 cm^{-1} was attributed to C–S and S=O vibrations, further supporting the contribution of sulfur–oxygen bonds in the polymeric backbone [42,45].

When compared with the irradiated sample (PFOS-I), a marked decrease in band intensity was observed, particularly in the CF_2 (368 and 714 cm^{-1}) and $SO_2/–CF_2/–CF_3$ (1207 cm^{-1}) regions, indicating partial degradation or structural rearrangement of these groups upon irradiation. This attenuation is likely due to C–F bond cleavage and the reduced symmetry of sulfonic moieties, a well-documented phenomenon in irradiated fluoropolymers. Notably, the 1329 cm^{-1} peak (C–S/S=O) also exhibited relative attenuation, suggesting that irradiation impacts both fluoroalkyl domains and sulfur-containing bonds, possibly via photoinduced oxidation mechanisms [44,46,47].

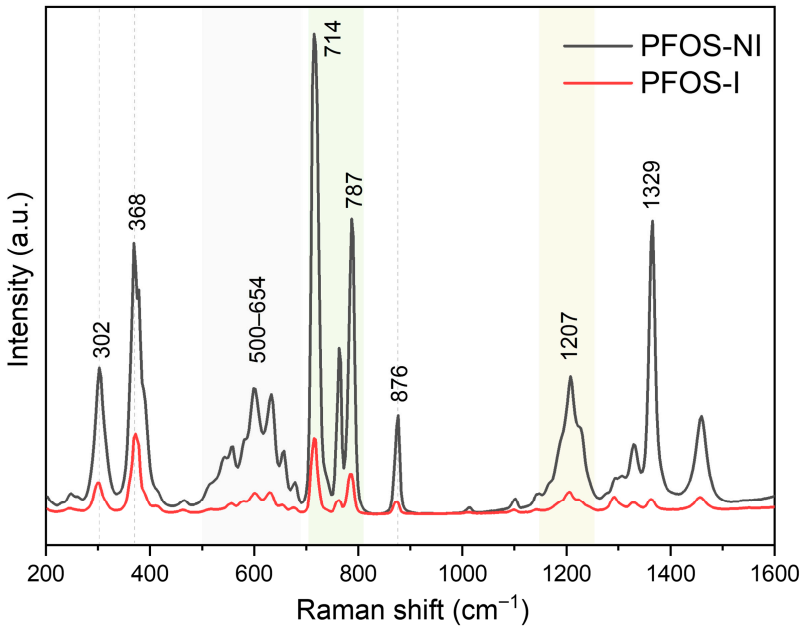


Figure 1. Raman spectra of PFOS non-irradiated (PFOS-NI, black) and irradiated (PFOS-I, red) samples highlight the characteristic bands assigned to fluorinated and sulfonated functional groups. The shaded regions indicate specific vibrational domains: the gray region (~300–654 cm^{-1}) corresponds to vibrational modes associated primarily with C–S and S–O stretching and CF_x bending; the green region (~700–800 cm^{-1}) denotes intense CF_3 and CF_2 stretching vibrations characteristic of fluorinated moieties; and the yellow region (~1150–1250 cm^{-1}) encompasses SO_3 symmetric and asymmetric stretching vibrations indicative of sulfonate functional groups. These spectral regions exhibit notable changes upon irradiation, reflecting structural modifications of PFOS.

3.2. Powder PFOS-FTIR

The FTIR spectrum of powdered PFOS (Figure 2) reflects the interplay between its perfluorinated backbone and sulfonated groups. A broad band between 3680–3000 cm^{-1}, assigned to ν(O–H) stretching of adsorbed water and strong hydrogen bonding with –SO_3H, becomes markedly more intense after irradiation, indicating the generation of polar functionalities that enhance hygroscopicity. The disappearance of the ~1770 cm^{-1} carbonyl peak suggests consumption of strained C=O intermediates, plausibly by further oxidation toward final mineralization products, as described in radiolytic perfluoroalkyl degradation. Meanwhile, the persistent ~1700 cm^{-1} band confirms the stable formation of carboxylic acids, a fingerprint of partial chain oxidation [43,46,48].

Characteristic C–F stretching bands (1250–1100 cm^{-1}) decrease in relative intensity after irradiation, consistent with progressive C–F bond cleavage and sulfonic group modification (–SO_3H → –SO_3^-), in line with mechanochemical and radiolytic pathways [49]. The ~1013 cm^{-1} peak, corresponding to ν_s(SO_3), shows intensity changes indicative of protonation loss and partial transformation to inorganic sulfates. Alterations in the fingerprint region (845–600 cm^{-1}), including O–S–O and CF_2 deformations, reflect loss of local order, sulfur oxidation, and product formation. Finally, attenuation of the 528–557 cm^{-1} doublet points to restructuring of sulfonate groups, including possible oxidation to sulfate [43,48].

In summary, irradiation drives powdered PFOS toward higher hydrophilicity, consumption of carbonyl intermediates, C–F cleavage, and sulfonate reorganization, all features characteristic of perfluoroalkyl destructive pathways [50]. The behavior of powdered PFOS after irradiation reveals increased surface hydration, consumption/transmutation of carbonyl intermediates, and progressive loss of C–F signatures along with sulfonate group reorganization, consistent with perfluoroalkyl destruction.

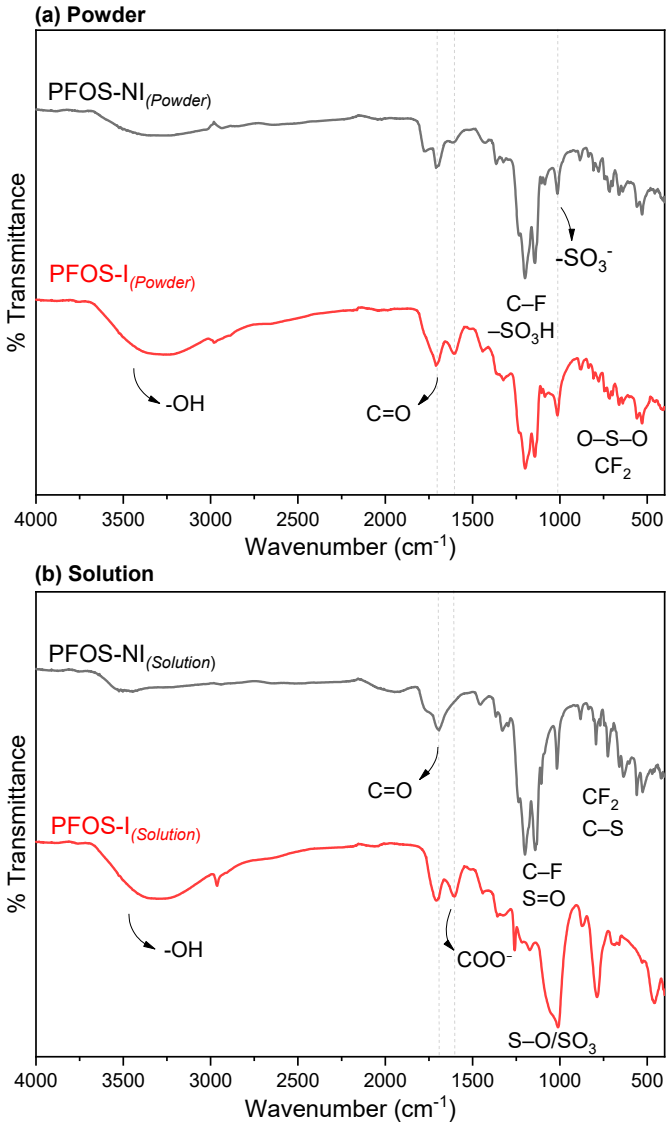


Figure 2. Comparative FTIR spectra of PFOS-I and PFOS-NI in (**a**) powder and (**b**) solution form, showing spectral differences associated with chemical modifications upon irradiation. The grey-shaded regions highlight key vibrational domains: the broad band around ~3200–3600 cm^{-1} corresponds to O–H stretching (indicative of hydroxyl group formation), the ~1100–1300 cm^{-1} region includes strong absorptions associated with C–F and S=O stretching vibrations, and the ~1000–1150 cm^{-1} range represents contributions from S–O/SO_3 modes. The dashed vertical lines emphasize the spectral positions where pronounced changes occur in the C–F and S=O stretching regions, indicating the disruption or transformation of fluorinated and sulfonated functional groups upon irradiation.

3.3. Solution of PFO in Water-FTIR

In the FTIR spectrum of PFO in solution (Figure 2), the main changes reflect both solvation and radiation-induced oxidation. The broad band at ~3660–3000 cm^{-1} (ν(O–H)) becomes more intense than in the solid state and further increases after irradiation, due to hydration and the formation of polar groups (–OH, –COOH) from oxidation of the perfluorinated backbone, consistent with hydration studies of perfluorosulfonates [49].

In the carbonyl region, a band at ~1690 cm^{-1} (ν(C=O)) appears together with a new feature at ~1605 cm^{-1} after irradiation, assigned to ν_as(COO^-) of carboxylates and/or water bending modes under strong association. This coexistence indicates radiolytic pathways producing both carbonyl intermediates and carboxylates prior to mineralization [51].

Characteristic C–F and S=O bands at 1200 and 1140 cm^{-1} merge into a broad feature at ≈1019 cm^{-1} post-irradiation, reflecting C–F cleavage and enhanced S–O/ν_s(SO_3) contributions or new oxygenated species. Likewise, the ≈818–700 cm^{-1} region, originally resolved into CF_2 wagging and C–S modes, collapses into a single broad band, indicating chemical fragmentation and homogenization of vibrational environments [48,50].

A general shift of vibrational bands toward higher wavenumbers was observed in irradiated solutions, suggesting an increase in bond stiffness and reduced anharmonicity. Such spectral trends are consistent with previous observations of irradiated fluorinated systems [47,51]. The shift is thought to emerge from ionization-induced electronic redistribution and enhanced solvation effects, which collectively strengthen local bonding environments and alter vibrational frequencies.

Overall, irradiation of PFOS solutions promote oxidation, carboxylate formation, C–F bond scission, and reorganization of S–O modes, leading to spectral broadening and loss of resolution in line with perfluoroalkyl radiolytic mineralization.

3.4. Cell Viability Assay

Treatment with both irradiated and non-irradiated PFOS solutions led to differences in the viability of human fibroblast cells compared to the positive control (DMEM-High). Notably, non-irradiated PFOS caused a significant reduction in cell viability at concentrations of 100 and 50 μg/mL ($p < 0.05$). In contrast, following neutron irradiation in the Argonauta Reactor, previously cytotoxic concentrations no longer induced cell death, showing viability levels comparable to the positive control (Figure 3). These results suggest that neutron-induced radiolysis triggered molecular alterations substantial enough to attenuate PFOS cytotoxicity, suggesting partial structural degradation of the compound in aqueous solution.

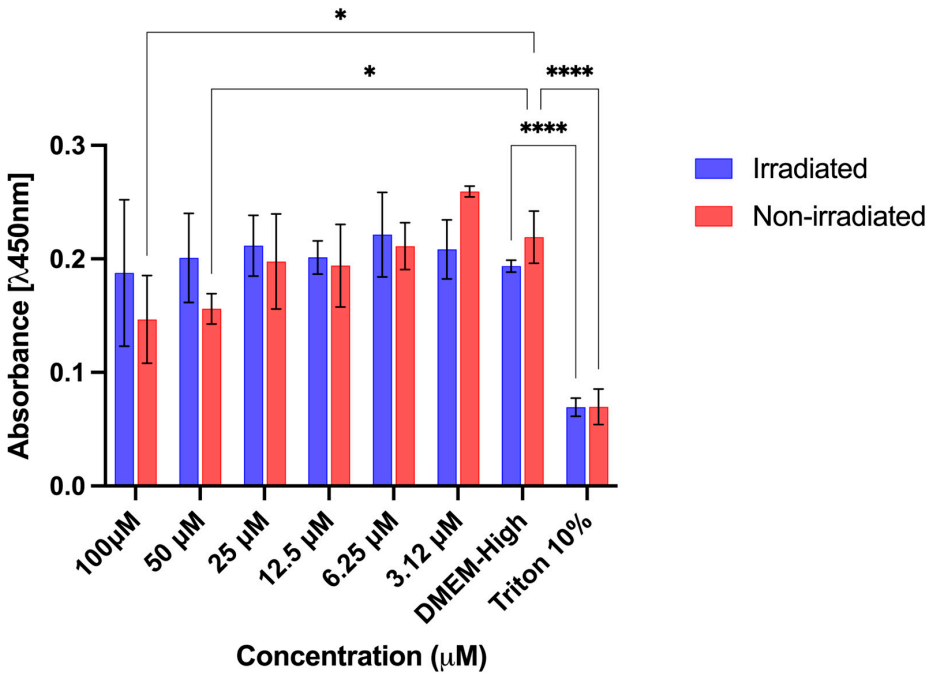


Figure 3. Effect of irradiated and non-irradiated perfluorooctane sulfonate (PFOS) solutions on the viability of human umbilical vein endothelial cells. Cells were exposed for 24 h to increasing concentrations of PFOS (3.125, 6.25, 12.5, 25, 50 and 100 μg/mL). Cell viability was assessed using the MTT assay, with absorbance measured at 450 nm and expressed relative to the untreated control. Data are presented as mean ± standard deviation (SD) from independent experiments ($n = 4$). Statistical analysis was performed using ANOVA, and significant differences between irradiated and non-irradiated PFOS treatments were observed at concentrations of 50 and 100 μg/mL. Significance levels are indicated as * $p < 0.05$ and **** $p < 0.0001$.

4. Discussion

4.1. Mechanistic Insights and Environmental Implications

Matrix-specific results point to a dual mechanistic paradigm: (i) in the solid state, neutron interactions are dominated by nuclear scattering and limited capture, which do not induce significant molecular degradation [52]; (ii) in aqueous solution, neutron- and γ-induced radiolysis chemistry enables bond cleavage and partial mineralization [50]. This distinction has direct implications for remediation strategies: while neutron-based approaches are likely ineffective for PFOS in soils or dry sediments, they may be promising for contaminated waters, particularly in localized hotspots such as firefighting training sites where PFOS concentrations are elevated. Table 1 summarizes the main mechanistic and techniques used.

Table 1. Benchmark of destructive PFOS treatment approaches reported in the literature and the present work.

Approach	Typical Reported Outcome (PFOS)	Key Constraints	Reference
Alkaline ozonation	~85–100% degradation within ~1 h (optimized lab conditions)	Chemistry-dependent; may be limited outside optimized conditions	[53]
Sonochemical (high-frequency cavitation)	~96.9% degradation after 4 h (optimized)	High energy demand; scale-up challenges	[54]
Plasma treatment	>50% degradation within <300 s (bench scale)	Reactor/energy efficiency; scalability	[26]
Electrochemical oxidation (pilot-scale; foam fractionation + EO)	~96% PFOS removal after 2 h (concentrated foam stream)	Electrode durability; energy; suited to point sources	[55]
This study: neutron irradiation (aqueous PFOS)	Spectroscopic transformation + loss of cytotoxicity at 50–100 µg/mL; matrix-dependent	Mineralization not quantified; requires radiological infrastructure	

Is important to notice that, in aqueous systems, PFOS transformation is consistent with reactive species generated by radiolysis in the reactor mixed-field environment (neutrons accompanied by prompt/secondary γ radiation), whereas in the solid state the dominant interaction is scattering with limited chemical consequence under the tested conditions

From an environmental perspective, the observed partial degradation implies the generation of more polar and soluble fragments, with greater mobility and potentially increased bioaccessibility. Although complete mineralization to CO_2 and F^- requires more severe energetic conditions, the loss of C–F signatures and the transient emergence of carbonyls/carboxylates provide strong evidence of transformation pathways relevant to PFOS environmental fate and persistence.

The reduction in PFOS cytotoxicity following neutron irradiation can be mechanistically explained by radiolysis-driven molecular transformations occurring in aqueous media. Such modifications increase the hydrophilicity of the molecules and reduce their surfactant-like interaction with lipid membranes and intracellular proteins. Consequently, the radiolytically modified PFOS exhibits diminished affinity for cellular membranes and decreased potential to disrupt mitochondrial function, resulting in a measurable recovery of cell viability in vitro.

Together, these findings indicate that neutron-induced radiolysis produces measurable chemical transformation signatures (FTIR/Raman) and concomitantly attenuates PFOS biological activity in aqueous media. Because ^{19}F NMR and quantitative defluorination metrics were not obtained here, future work will verify transformation pathways and mass balance using LC–MS/MS, F^- quantification, TOC, and ^{19}F NMR. [24,56,57]. This pattern is consistent with radiolysis-driven conversion of amphiphilic PFOS into more oxygenated, less membrane-active species, thereby reducing cellular stress pathways commonly associ-

ated with PFAS exposure. Finally schematic summary of the proposed aqueous radiolysis pathway linking neutron irradiation to PFOS transformation and reduced cytotoxicity is provided in Figure 4.

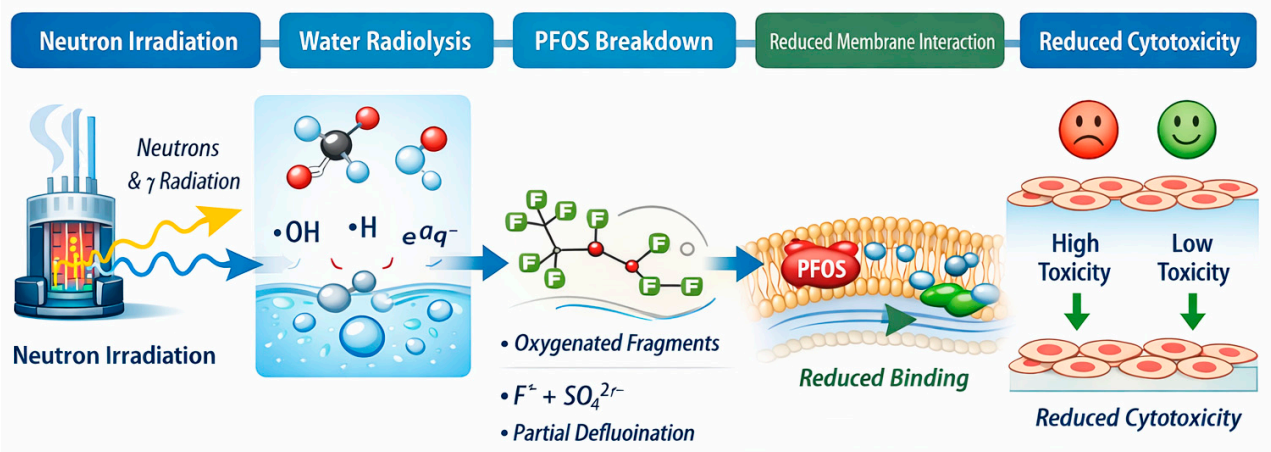


Figure 4. Proposed mechanism for PFOS detoxification under neutron irradiation in aqueous media: neutron-driven water radiolysis generates reactive species (•OH, •H, e_aq$^-$) that promote C–F/S–O bond transformations, formation of oxygenated fragments/partial defluorination, decreased surfactant-like membrane interaction, and attenuation of cytotoxicity in HUVEC cells.

4.2. Limitations and Future Directions

The observed degradation in solution, while reproducible, remained incomplete under the present conditions. Enhanced efficacy may be achievable at higher neutron fluxes, longer exposure times, or through synergistic methods combining irradiation with radical sensitizers or catalytic substrates that promote electron transfer [58]. Furthermore, the formation of shorter chain perfluoroalkyl intermediates necessitates comprehensive transformation product monitoring, given their own persistence and potential toxicity.

Future studies should therefore quantify defluorination yields, characterize transformation product spectra, and assess scalability to environmentally relevant concentrations. They must also enable mass-balance assessment of degradation versus detoxification through the use of quantitative analytics. Techniques include LC–MS/MS for parent PFOS and transformation products, ion chromatography for released F^-, TOC for mineralization tracking, and ^{19}F NMR to probe fluorinated-fragment evolution.

To enable direct benchmarking against established destructive technologies (e.g., γ-irradiation, electron beam, electrochemical oxidation, plasma), future work will quantify PFOS concentration and transformation products using validated analytical workflows (e.g., LC–MS/MS for PFOS and by-products, ion chromatography for released F^-/SO_4^{2-}, and TOC for mineralization), and will normalize outcomes to absorbed dose (Gy) to derive energy-specific degradation metrics

In addition, future studies will incorporate optical and fluorescence microscopy analyses to provide qualitative morphological assessment and visual confirmation of cellular responses to irradiated and non-irradiated PFOS treatments, thereby complementing the quantitative cell viability data obtained in the present work.

Radiological practicality and matrix activation are critical considerations for any neutron-based approach. Radioactivation is highly matrix-dependent: dissolved salts, metals, and soil/mineral components can form activation products under neutron exposure, potentially converting treated material into regulated radioactive waste. Accordingly, the present study is positioned as a controlled proof-of-concept focused on mechanistic transformation and biological activity attenuation in simplified matrices (solid PFOS and

aqueous PFOS). Translation to real environmental samples would require (i) gamma spectrometric assessment of induced activity, (ii) matrix pre-treatment or selection strategies to minimize activation-prone constituents, and (iii) implementation only in contained, ex situ treatment settings with appropriate radiological controls

5. Conclusions

This study provides the first integrated physicochemical and biological evaluation of PFOS degradation induced by neutron irradiation. A clear matrix-dependent behavior was demonstrated: while PFOS in the solid state remained largely resistant to neutron exposure, aqueous PFOS underwent radiolysis-driven molecular transformation characterized by attenuation of C–F and S–O vibrational signatures and the emergence of oxygenated functional groups. These spectroscopic changes provide direct evidence of partial defluorination and oxidative restructuring mediated by water radiolysis products.

Crucially, the chemical transformation observed in aqueous systems translated into a marked biological effect. Neutron-irradiated PFOS solutions no longer exhibited cytotoxicity toward human endothelial cells at concentrations that were highly toxic in the non-irradiated form, demonstrating that neutron-induced radiolysis effectively suppresses PFOS biological activity. This coupling of molecular degradation with functional toxicological recovery represents a key original contribution of this study.

The novelty of this study lies in establishing neutron irradiation as a distinct and mechanistically grounded pathway for PFOS detoxification in water, bridging nuclear chemistry, environmental spectroscopy, and cellular toxicology. While complete mineralization was not achieved under the present conditions, the results provide a strong proof of concept and a foundation for future optimization of neutron flux, irradiation time, and synergistic catalytic systems. Overall, this work positions neutron-assisted radiolysis as a promising, albeit specialized, strategy for the treatment of PFOS-contaminated aqueous environments.

Author Contributions: Conceptualization, R.S.-O.; methodology, J.I.F.d.S., P.B.A.F. and L.M.R.A.; investigation, J.I.F.d.S. and J.F.d.C.A.; formal analysis, E.R.-J. and S.A.J.; writing—original draft preparation, J.I.F.d.S. and R.S.-O.; writing—review and editing, all authors; supervision, R.S.-O. All authors have read and agreed to the published version of the manuscript.

Funding: This study was funded by Carlos Chagas Filho Foundation for Research Support of Rio de Janeiro State (FAPERJ) (Cientista do Nosso Estado: E-26/200.815/2021; Rede NanoSaude: E-26/010.000981/2019, Pesquisa na UEZO: E-26/010.002362/2019; Temáticos: E-26/211.269/2021, Infraestrutura e Pesquisa na UEZO e UERJ: E-26//211.207/2021, Bolsa de Pós-doutorado Senior (PDS): E-26/202.320/2021) and CNPq (Bolsa de Produtividade 1B: 301069/2018-2) to Ralph Santos-Oliveira, (Bolsa de Produtividade 2: 304774/2021-9) to Luciana Alencar, Universal (401692/2023-0), Internacional (440852/2023-4) and CNPq/Ministerio da Saude-Medicina de Precisão (444089/2023). Finally, this study was supported by Brazilian and Chilean agencies: CNPq (308452/2022–4), CAPES (Finance Code 001—PROEX 23038.000509/2020–82).

Data Availability Statement: All data will be available under request.

Acknowledgments: The authors thank all researchers and collaborators for their valuable scientific contributions and discussions. During the preparation of this manuscript, LanguageTool for Desktop (version 2.9.5) was used solely for grammar checking and language correction. The authors reviewed and edited all AI-assisted content and take full responsibility for this publication.

Conflicts of Interest: The authors state that they have no conflict of interest.

References

1. Chang, M.; Yin, R.; Wang, J.; You, M.; Wang, N.; Wong, Y.J.; Xiao, T. Perfluorooctane Sulfonate (PFOS) and Perfluorooctanoic Acid (PFOA) in the Surface Waters of China: A Meta-Analysis. *Water* **2025**, *17*, 1275. [CrossRef]
2. Mazumder, N.-U.-S.; Hossain, M.T.; Jahura, F.T.; Girase, A.; Hall, A.S.; Lu, J.; Ormond, R.B. Firefighters' Exposure to per-and Polyfluoroalkyl Substances (PFAS) as an Occupational Hazard: A Review. *Front. Mater.* **2023**, *10*, 1143411. [CrossRef]
3. Kane, D.L.; Figula, B.C.; Balaraman, K.; Bertke, J.A.; Wolf, C. Cryogenic Organometallic Carbon–Fluoride Bond Functionalization with Broad Functional Group Tolerance. *J. Am. Chem. Soc.* **2025**, *147*, 5764–5774. [CrossRef]
4. Pan, C.-G.; Sun, R.-X. Understanding PFAS: Occurrence, Fate, Removal, and Effects. *Toxics* **2024**, *12*, 605. [CrossRef]
5. Krafft, M.P. From Fluorine's Position in the Periodic Table to PFAS Environmental Issues. *Comptes Rendus. Chim.* **2025**, *28*, 423–438. [CrossRef]
6. Cara, B.; Lies, T.; Thimo, G.; Robin, L.; Lieven, B. Bioaccumulation and Trophic Transfer of Perfluorinated Alkyl Substances (PFAS) in Marine Biota from the Belgian North Sea: Distribution and Human Health Risk Implications. *Environ. Pollut.* **2022**, *311*, 119907. [CrossRef] [PubMed]
7. Cao, L.; Guo, Y.; Chen, Y.; Hong, J.; Wu, J.; Jin, H. Per-/Polyfluoroalkyl Substance Concentrations in Human Serum and Their Associations with Liver Cancer. *Chemosphere* **2022**, *296*, 134083. [CrossRef]
8. Cai, Z.; Zhou, G.; Yu, X.; Du, Y.; Man, Q.; Wang, W.C. Perfluorooctanoic Acid Disrupts Thyroid Hormone Biosynthesis by Altering Glycosylation of Na+/I− Symporter in Larval Zebrafish. *Ecotoxicol. Environ. Saf.* **2025**, *297*, 118249. [CrossRef] [PubMed]
9. Hua, W.; Yang, R.; Alam, M.N.; Che, Z.; Zhu, W.; Tian, M.; Lu, Y.-Y.; Sun, Y.; Huang, Q. Perfluorooctane Sulfonate Exposure Disrupts Steroid Hormone Synthesis in Rats via the Gut-Metabolism-Testis Axis. *Environ. Pollut.* **2025**, *381*, 126594. [CrossRef]
10. Qiu, J.; Huo, X.; Dai, Y.; Huang, Y.; Xu, X. Potential Effects of PFAS Exposure on Trained Immunity: From Mechanisms to Health Risks. *Ecotoxicol. Environ. Saf.* **2025**, *302*, 118757. [CrossRef] [PubMed]
11. Kashobwe, L.; Sadrabadi, F.; Brunken, L.; Coelho, A.C.M.F.; Sandanger, T.M.; Braeuning, A.; Buhrke, T.; Öberg, M.; Hamers, T.; Leonards, P.E.G. Legacy and Alternative Per- and Polyfluoroalkyl Substances (PFAS) Alter the Lipid Profile of HepaRG Cells. *Toxicology* **2024**, *506*, 153862. [CrossRef] [PubMed]
12. Fragki, S.; Dirven, H.; Fletcher, T.; Grasl-Kraupp, B.; Bjerve Gützkow, K.; Hoogenboom, R.; Kersten, S.; Lindeman, B.; Louisse, J.; Peijnenburg, A.; et al. Systemic PFOS and PFOA Exposure and Disturbed Lipid Homeostasis in Humans: What Do We Know and What Not? *Crit. Rev. Toxicol.* **2021**, *51*, 141–164. [CrossRef] [PubMed]
13. Zuo, X.; Tan, S.; Zhang, Y.; Zhang, C.; Ma, L.; Hou, X.; Wang, W.; Sun, R.; Yin, L.; Pu, Y.; et al. Linking PFOS Exposure to Chronic Kidney Disease: A Multimodal Study Integrating Epidemiology, Network Toxicology, and Experimental Validation. *Ecotoxicol. Environ. Saf.* **2025**, *302*, 118770. [CrossRef]
14. Fenton, S.E.; Ducatman, A.; Boobis, A.; DeWitt, J.C.; Lau, C.; Ng, C.; Smith, J.S.; Roberts, S.M. Per- and Polyfluoroalkyl Substance Toxicity and Human Health Review: Current State of Knowledge and Strategies for Informing Future Research. *Environ. Toxicol. Chem.* **2021**, *40*, 606–630. [CrossRef] [PubMed]
15. EFSA Panel on Contaminants in the Food Chain (CONTAM); Knutsen, H.K.; Alexander, J.; Barregård, L.; Bignami, M.; Brüschweiler, B.; Ceccatelli, S.; Cottrill, B.; Dinovi, M.; Edler, L.; et al. Risk to Human Health Related to the Presence of Perfluorooctane Sulfonic Acid and Perfluorooctanoic Acid in Food. *EFS2* **2018**, *16*, e05194. [CrossRef]
16. The Stockholm Convention on Persistent Organic Pollutants All POPs Listed in the Stockholm Convention. Available online: https://www.pops.int/TheConvention/ThePOPs/AllPOPs/tabid/2509/Default.aspx (accessed on 11 October 2025).
17. Kurwadkar, S.; Dane, J.; Kanel, S.R.; Nadagouda, M.N.; Cawdrey, R.W.; Ambade, B.; Struckhoff, G.C.; Wilkin, R. Per- and Polyfluoroalkyl Substances in Water and Wastewater: A Critical Review of Their Global Occurrence and Distribution. *Sci. Total Environ.* **2022**, *809*, 151003. [CrossRef]
18. Environment Agency. *Poly- and Perfluoroalkyl Substances (PFAS): Sources, Pathways and Environmental Data*; [Internet]; Environment Agency: London, UK, 26 August 2021. Available online: https://www.gov.uk/government/publications/poly-and-perfluoroalkyl-substances-pfas-sources-pathways-and-environmental-data (accessed on 11 October 2025).
19. Thompson, K.A.; Mortazavian, S.; Gonzalez, D.J.; Bott, C.; Hooper, J.; Schaefer, C.E.; Dickenson, E.R.V. Poly- and Perfluoroalkyl Substances in Municipal Wastewater Treatment Plants in the United States: Seasonal Patterns and Meta-Analysis of Long-Term Trends and Average Concentrations. *ACS EST Water* **2022**, *2*, 690–700. [CrossRef]
20. Bhattacharya, A.; Fathima, J.; Varghese, S.; Chatterjee, P.; Gadhamshetty, V. Advances in Bioremediation Strategies for PFAS-Contaminated Water and Soil. *Soil Environ. Health* **2025**, *3*, 100126. [CrossRef]
21. Sanzana, S.; Fenti, A.; Iovino, P.; Panico, A. A Review of PFAS Remediation: Separation and Degradation Technologies for Water and Wastewater Treatment. *J. Water Process Eng.* **2025**, *74*, 107793. [CrossRef]
22. Mukonza, S.S.; Chaukura, N. Bird's-Eye View of per- and Polyfluoroalkyl Substances Pollution Research in the African Hydrosphere. *npj Clean Water* **2025**, *8*, 67. [CrossRef]
23. Dimitrakopoulou, M.-E.; Karvounis, M.; Marinos, G.; Theodorakopoulou, Z.; Aloizou, E.; Petsangourakis, G.; Papakonstantinou, M.; Stoitsis, G. Comprehensive Analysis of PFAS Presence from Environment to Plate. *npj Sci. Food* **2024**, *8*, 80. [CrossRef]

24. Malouchi, N.; Chatzimichailidou, S.; Tolkou, A.K.; Kyzas, G.Z.; Calgaro, L.; Marcomini, A.; Katsoyiannis, I.A. The Removal of Per- and Poly-Fluoroalkyl Substances from Water: A Review on Destructive and Non-Destructive Methods. *Separations* **2024**, *11*, 122. [CrossRef]
25. Kumari, P.; Kumar, A. ADVANCED OXIDATION PROCESS: A Remediation Technique for Organic and Non-Biodegradable Pollutant. *Results Surf. Interfaces* **2023**, *11*, 100122. [CrossRef]
26. Smith, S.J.; Lauria, M.; Ahrens, L.; McCleaf, P.; Hollman, P.; Bjälkefur Seroka, S.; Hamers, T.; Arp, H.P.H.; Wiberg, K. Electrochemical Oxidation for Treatment of PFAS in Contaminated Water and Fractionated Foam—A Pilot-Scale Study. *ACS EST Water* **2023**, *3*, 1201–1211. [CrossRef] [PubMed]
27. Alsadik, A.; Akintunde, O.O.; Habibi, H.R.; Achari, G. PFAS in Water Environments: Recent Progress and Challenges in Monitoring, Toxicity, Treatment Technologies, and Post-Treatment Toxicity. *Environ. Syst. Res.* **2025**, *14*, 18. [CrossRef]
28. Winchell, L.J.; Ross, J.J.; Wells, M.J.M.; Fonoll, X.; Norton, J.W.; Bell, K.Y. Per- and Polyfluoroalkyl Substances Thermal Destruction at Water Resource Recovery Facilities: A State of the Science Review. *Water Environ. Res.* **2021**, *93*, 826–843. [CrossRef]
29. Inoue, Y.; Hashizume, N.; Yakata, N.; Murakami, H.; Suzuki, Y.; Kikushima, E.; Otsuka, M. Unique Physicochemical Properties of Perfluorinated Compounds and Their Bioconcentration in Common Carp *Cyprinus carpio* L. *Arch. Environ. Contam. Toxicol.* **2012**, *62*, 672–680. [CrossRef] [PubMed]
30. Leung, S.C.E.; Wanninayake, D.; Chen, D.; Nguyen, N.-T.; Li, Q. Physicochemical Properties and Interactions of Perfluoroalkyl Substances (PFAS)—Challenges and Opportunities in Sensing and Remediation. *Sci. Total Environ.* **2023**, *905*, 166764. [CrossRef]
31. Fatima, M.; Kelso, C.; Hai, F. Perfluorooctanoic Acid (PFOA) and Perfluorooctanesulfonic Acid (PFOS) Adsorption onto Different Adsorbents: A Critical Review of the Impact of Their Chemical Structure and Retention Mechanisms in Soil and Groundwater. *Water* **2025**, *17*, 1401. [CrossRef]
32. Ochoa-Herrera, V.; Field, J.A.; Luna-Velasco, A.; Sierra-Alvarez, R. Microbial Toxicity and Biodegradability of Perfluorooctane Sulfonate (PFOS) and Shorter Chain Perfluoroalkyl and Polyfluoroalkyl Substances (PFASs). *Environ. Sci. Process. Impacts* **2016**, *18*, 1236–1246. [CrossRef]
33. Awoyemi, O.S.; Naidu, R.; Fang, C. Advancements on Ultrasonic Degradation of Per- and Polyfluoroalkyl Substances (PFAS): Toward Hybrid Approaches. *Environments* **2024**, *11*, 187. [CrossRef]
34. Niu, S.; Gong, X.; Li, Z.; Sun, Y.; Lyu, H. Degradation of Perfluoroalkyl and Polyfluoroalkyl Substances in Soils and Water. In *Adsorption and Degradation of Emerging Contaminants in Soils and Water*; Elsevier: Amsterdam, The Netherlands, 2026; pp. 133–200, ISBN 978-0-443-33046-9.
35. Khene, S. Atoms. In *Topics and Solved Exercises at the Boundary of Classical and Modern Physics; Undergraduate Lecture Notes in Physics*; Springer International Publishing: Cham, The Netherlands, 2021; pp. 1–132, ISBN 978-3-030-87741-5.
36. Kiragga, F.; Brazovskiy, K. Exploiting the Unique Interaction Characteristics of Fast Neutrons for Improved Cancer Therapy: A Radiobiological Perspective. *Radiat. Med. Prot.* **2024**, *5*, 24–29. [CrossRef]
37. Cameron, I.R. *Nuclear Fission Reactors*; Springer: Boston, MA, USA, 1982; ISBN 978-1-4613-3529-0.
38. Yang, W.; Dong, F. Degradation Breakthrough of Stabilized Compounds with C-F Bonds. *Innov. Mater.* **2025**, *3*, 100142. [CrossRef]
39. Jay-Gerin, J.-P. Fundamentals of Water Radiolysis. *Encyclopedia* **2025**, *5*, 38. [CrossRef]
40. Alencar, L.M.R.; Rates, E.R.D.; Gomes-da-Silva, N.C.; Pijeira, M.S.O.; Teixeira, B.N.; Golokhvast, K.; Ricci-Junior, E.; Thiré, R.M.D.S.M.; Santos-Oliveira, R. Polymeric Nanoparticles Mimicking Microplastics/Nanoplastics: Ultrastructural and Rheological Analysis of the Effect of Neutrons on Their Structures. *Environ. Nanotechnol. Monit. Manag.* **2023**, *20*, 100876. [CrossRef]
41. Singh, R.; Kesharwani, P.; Mehra, N.K.; Singh, S.; Banerjee, S.; Jain, N.K. Development and Characterization of Folate Anchored Saquinavir Entrapped PLGA Nanoparticles for Anti-Tumor Activity. *Drug Dev. Ind. Pharm.* **2015**, *41*, 1888–1901. [CrossRef]
42. Kumar, A.; Rothstein, J.C.; Chen, Y.; Zhang, H.; Zhao, Y. Experimental Raman Spectra Analysis of Selected PFAS Compounds: Comparison with DFT Predictions. *J. Hazard. Mater.* **2025**, *494*, 138704. [CrossRef]
43. Socrates, G. *Infrared and Raman Characteristic Group Frequencies: Tables and Charts*; John Wiley & Sons: Hoboken, NJ, USA, 2004; ISBN 978-0-470-09307-8.
44. Edwards, H.G.M. Spectra–Structure Correlations in Raman Spectroscopy. In *Handbook of Vibrational Spectroscopy*; John Wiley & Sons, Ltd.: Hoboken, NJ, USA, 2006; ISBN 978-0-470-02732-5.
45. Cho, S.; Remucal, C.K.; Wei, H. Common and Distinctive Raman Spectral Features for the Identification and Differentiation of Per- and Polyfluoroalkyl Substances. *ACS EST Water* **2025**, *5*, 300–309. [CrossRef]
46. Patch, D.; O'Connor, N.; Koch, I.; Cresswell, T.; Hughes, C.; Davies, J.B.; Scott, J.; O'Carroll, D.; Weber, K. Elucidating Degradation Mechanisms for a Range of Per- and Polyfluoroalkyl Substances (PFAS) via Controlled Irradiation Studies. *Sci. Total Environ.* **2022**, *832*, 154941. [CrossRef] [PubMed]
47. Feng, M.; Gao, R.; Staack, D.; Pillai, S.D.; Sharma, V.K. Degradation of Perfluoroheptanoic Acid in Water by Electron Beam Irradiation. *Environ. Chem. Lett.* **2021**, *19*, 2689–2694. [CrossRef]
48. Zhang, K.; Huang, J.; Yu, G.; Zhang, Q.; Deng, S.; Wang, B. Destruction of Perfluorooctane Sulfonate (PFOS) and Perfluorooctanoic Acid (PFOA) by Ball Milling. *Environ. Sci. Technol.* **2013**, *47*, 6471–6477. [CrossRef]

49. Agarwal, T.; Prasad, A.K.; Advani, S.G.; Babu, S.K.; Borup, R.L. Infrared Spectroscopy for Understanding the Structure of Nafion and Its Associated Properties. *J. Mater. Chem. A* **2024**, *12*, 14229–14244. [CrossRef]
50. Zhang, Z.; Chen, J.-J.; Lyu, X.-J.; Yin, H.; Sheng, G.-P. Complete Mineralization of Perfluorooctanoic Acid (PFOA) by γ-Irradiation in Aqueous Solution. *Sci. Rep.* **2014**, *4*, 7418. [CrossRef] [PubMed]
51. Deng, Y.; Liang, Z.; Lu, X.; Chen, D.; Li, Z.; Wang, F. The Degradation Mechanisms of Perfluorooctanoic Acid (PFOA) and Perfluorooctane Sulfonic Acid (PFOS) by Different Chemical Methods: A Critical Review. *Chemosphere* **2021**, *283*, 131168. [CrossRef]
52. Snow, W.M.; Haddock, C.; Heacock, B. Searches for Exotic Interactions Using Neutrons. *Symmetry* **2021**, *14*, 10. [CrossRef]
53. Lin, A.Y.-C.; Panchangam, S.C.; Chang, C.-Y.; Hong, P.K.A.; Hsueh, H.-F. Removal of Perfluorooctanoic Acid and Perfluorooctane Sulfonate via Ozonation under Alkaline Condition. *J. Hazard. Mater.* **2012**, *243*, 272–277. [CrossRef]
54. Huang, J.; Wang, X.; Pan, Z.; Li, X.; Ling, Y.; Li, L. Efficient Degradation of Perfluorooctanoic Acid (PFOA) by Photocatalytic Ozonation. *Chem. Eng. J.* **2016**, *296*, 329–334. [CrossRef]
55. James Wood, R.; Sidnell, T.; Ross, I.; McDonough, J.; Lee, J.; Bussemaker, M.J. Ultrasonic Degradation of Perfluorooctane Sulfonic Acid (PFOS) Correlated with Sonochemical and Sonoluminescence Characterisation. *Ultrason. Sonochem.* **2020**, *68*, 105196. [CrossRef]
56. Windisch, M.; Klymenko, R.; Grießler, H.; Kittinger, C. Assessment of Cytotoxicity and Genotoxicity of Plasma-Treated Perfluorooctanesulfonate Containing Water Using In Vitro Bioassays. *Toxics* **2024**, *12*, 889. [CrossRef]
57. Trojanowicz, M.; Bartosiewicz, I.; Bojanowska-Czajka, A.; Szreder, T.; Bobrowski, K.; Nałęcz-Jawecki, G.; Męczyńska-Wielgosz, S.; Nichipor, H. Application of Ionizing Radiation in Decomposition of Perfluorooctane Sulfonate (PFOS) in Aqueous Solutions. *Chem. Eng. J.* **2020**, *379*, 122303. [CrossRef]
58. Kim, T.-H.; Lee, S.-H.; Kim, H.Y.; Doudrick, K.; Yu, S.; Kim, S.D. Decomposition of Perfluorooctane Sulfonate (PFOS) Using a Hybrid Process with Electron Beam and Chemical Oxidants. *Chem. Eng. J.* **2019**, *361*, 1363–1370. [CrossRef]

Disclaimer/Publisher's Note: The statements, opinions and data contained in all publications are solely those of the individual author(s) and contributor(s) and not of MDPI and/or the editor(s). MDPI and/or the editor(s) disclaim responsibility for any injury to people or property resulting from any ideas, methods, instructions or products referred to in the content.